②

AD-A228 814

RADC-TR-90-246
Final Technical Report
September 1990

INTRA-PULSE FREQUENCY DIVERSITY (IPFD) LAB DEMONSTRATION

Syracuse University

DTIC
S ELECTE D
NOV 26 1990
D

Dr. Hong Wang

APPROVED FOR PUBLIC RELEASE; DISTRIBUTION UNLIMITED.

**Rome Air Development Center
Air Force Systems Command
Griffiss Air Force Base, NY 13441-5700**

This report has been reviewed by the RADC Public Affairs Division (PA) and is releasable to the National Technical Information Services (NTIS) At NTIS it will be releasable to the general public, including foreign nations.
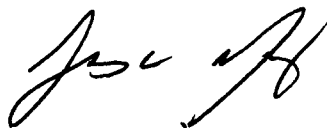
RADC-TR-90-246 has been reviewed and is approved for publication.
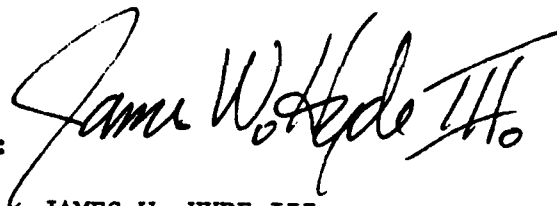
APPROVED:

VINCENT VANNICOLA
Project Engineer

APPROVED:

JAMES W. YOUNGBERG, LtCol, USAF
Deputy Director of Surveillance

FOR THE COMMANDER:

JAMES W. HYDE III
Directorate of Plans & Programs

REPORT DOCUMENTATION PAGE

Form Approved
OMB No. 0704-0188

1. AGENCY USE ONLY (Leave Blank)	2. REPORT DATE September 1990	3. REPORT TYPE AND DATES COVERED Final Jan 89 - Sep 89

4. TITLE AND SUBTITLE INTRA-PULSE FREQUENCY DIVERSITY (IPFD) LAB DEMONSTRATION	5. FUNDING NUMBERS C - F30602-88-D-0027 PE - 62702F PR - 4506 TA - 11 WU - P1
6. AUTHOR(S) Dr. Hong Wang	

7. PERFORMING ORGANIZATION NAME(S) AND ADDRESS(ES) Syracuse University Skytop Office Building Syracuse NY 13244-5300	8. PERFORMING ORGANIZATION REPORT NUMBER

9. SPONSORING/MONITORING AGENCY NAME(S) AND ADDRESS(ES) Rome Air Development Center (OCTS) Griffiss AFB NY 13441-5700	10. SPONSORING/MONITORING AGENCY REPORT NUMBER RADC-TR-90-246

11. SUPPLEMENTARY NOTES

RADC Project Engineer: Vincent Vannicola/OCTS/(315) 330-4437

12a. DISTRIBUTION/AVAILABILITY STATEMENT Approved for public release; distribution unlimited.	12b. DISTRIBUTION CODE

13. ABSTRACT (Maximum 200 words)

This correspondence suggests a new approach to wideband adaptive beamforming for correlated signal and interference. Unlike other approaches, such as spatial smoothing, the new approach solves the signal cancellation problem by employing the idea of frequency domain smoothing. Advantages of frequency domain smoothing method show that proper spatial filtering can be achieved by frequency domain smoothing, whether the desired signal and the interference are correlated or not.

14. SUBJECT TERMS Radar, Signal Processing, Spectral Estimation	15. NUMBER OF PAGES 24
	16. PRICE CODE

17. SECURITY CLASSIFICATION OF REPORT UNCLASSIFIED	18. SECURITY CLASSIFICATION OF THIS PAGE UNCLASSIFIED	19. SECURITY CLASSIFICATION OF ABSTRACT UNCLASSIFIED	20. LIMITATION OF ABSTRACT UL

I. THE DEMONSTRATION

Objective

Obtain higher resolution in the doppler frequency domain for improved target detectability in distributed clutter.

Approach

Intra-pulse frequency diversity waveform is used to increase the number of independent data samples for pulse-doppler processing without increasing the observation length. These independent data samples are coherently processed via the newly developed CUB-MFBLP method [1] to achieve a stable high-resolution doppler spectrum.

Data Acquisition and Processing

The RADC L-band facility and AP-120B array processor were used. See [2] for details of the waveform design, configuration and programs. Matrix operations were performed on the complex baseband radar data to provide coherent processing of the doppler spectrum by eigenvalue decomposition.

Contents of This Demonstration

(1)   The intra-pulse frequency diversity waveform which drives the L-band transmitter: three subpulses of three microsecond each with the carrier frequencies of -6, -1 and +4 MHz (with respect to the reference frequency).

(2)   The spectrum of the above waveform.

(3)   The range-doppler plot with the conventional FFT based pulse-doppler processing (8 pulses with rectangular window): the weak target in the range-extended strong clutter is not detectable since the doppler frequency separation is smaller than the Fourier resolution limit.

(4)   Same as (3) above with Hamming window for lower sidelobes: target is still not detectable.

(5)   The range-doppler plot with the new method: the target is clearly detectable.

(6)   The "zoomed-in" range-doppler plot with the new method.

References

[1]   H. Wang. and J.X. Zhu, "On Performance Improvement of Tone Frequency Estimation in Active Radar and Sonar Systems," to appear in IEEE Trans. on Acoustics, Speech, and Signal Processing, Vol. 36, No. 10, 1988.

[2]   Russell Brown and H. Wang, "High-Resolution Pulse-Doppler Processing with Intra-Pulse Frequency Diversity Waveform," RADC Tech. Report under preparation.

II. OTHER ACCOMPLISHMENTS

Journal Papers Submitted:

J.X. Zhu and H. Wang, "A comparison of smoothing approaches for angle measurement," to appear in IEEE Trans. on Aerspace and Electronic Systems Vol. AES-25, No. 4, July, 1989.

J.X. Zhu and H. Wang, "Adaptive beamforming for correlated signal and interference," to appear in IEEE Trans. on Acoustics, Speech and Signal Processing, Vol. ASSP. 37, 1989.

Conference Paper Published:

J.X. Zhu and H. Wang, "Effects of sensor position and pattern perturbations on CRLB for direction-finding of multiple narrow-band sources," Proc. 4th ASSP Workshop on Spectrum Estimation and Modeling, pp. 98-102, Minneapolis, MN, Aug. 3-5, 1988 (Invited).

Ph.D. Dissertation Completed:

C.C. Li, Active High-Resolution Multiple-Target Direction Finding, Syracuse University, 1988.

Copies of the above publications are attached.

A Comparison of Smoothing Approaches for Angle Measurement

JIAN-XIONG ZHU, Student, IEEE

HONG WANG, Member, IEEE
Syracuse University

For high-resolution active direction finding of completely correlated targets, one can use two approaches, i.e., the frequency-domain smoothing [1] and the non-frequency-domain smoothing such as various spatial smoothing [2-7], or multidimensional search of signal-subspace [8, 9]. A performance comparison of the two approaches for the fluctuating target cases under equal transmitted-energy constraint is presented. Both theoretical analysis and simulations are used to study the performance of the detection (determination of number of targets) and angle estimation. It is found that the frequency-domain smoothing can significantly outperform the non-frequency-domain smoothing under the equal transmitted-energy constraint.

I. INTRODUCTION

High-resolution direction finding of angularly closely spaced targets has received increasing attention in the past few years. Many methods have been suggested and are still under further investigation, e.g., MEM, MLM, MUSIC, modified FBLP (Min-Norm), ESPRIT, etc. Unfortunately, the detection, resolution, and estimation performances of these methods often suffer severe degradation in the cases of completely correlated target-signal returns caused by severe multipath or "smart" jamming.

The degradation can stem from the fact that the covariance matrix of the target signals is nearly singular or even completely singular. One class of methods to remove such singularity is the so-called spatial smoothing [2-7]. For example, the full sensor array can be divided into partially overlapping subarrays to average the covariance matrices of the subarray output vectors. It is obvious that such a spatial smoothing method can only be applied to the arrays with uniformly spaced identical sensors. Besides, a trade-off has to be made for a given array between the size of the subarrays and the number of subarrays, since the final performances depend on both parameters. Moreover, if the number of sensors is not large enough, the number of subarrays for the spatial smoothing might be too small to effectively remove the singularity. One can also easily see that such a spatial smoothing method does not make full use of the information contained in the data vectors since the off-diagonal blocks of the estimated covariance matrix are discarded. Other methods to solve the difficulty include the maximum likelihood parameter estimation [10], which in general requires a computationally extensive multidimensional search algorithm except in the case of the symmetric multipath, and the multidimensional search of signal-subspace [8, 9], which is also computationally demanding.

For active direction finding systems in which one has control of the transmitted waveform, Wang, Li, and Zhu [1] proposed the frequency-domain smoothing approach in contrast to the above mentioned methods which we refer to as non-frequency-domain smoothing. The frequency-domain smoothing approach is based on the use of frequency diversity signaling and the coherent processing idea which was originally developed in [11-13] for passive direction finding of wideband sources.

We present a performance comparison of the two approaches for active direction finding of completely correlated fluctuating targets using multiple observations (snapshots). A frequency diversity signaling with the equal transmitted-energy constraint is assumed for the frequency-domain smoothing in order to have a fair comparison. This paper is organized as follows. In Section II we set up the data-vector models for fluctuating
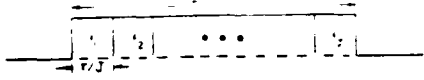
Fig. 1. Frequency diversity signaling pulse.

targets and introduce our notations. In Section III we compare the potential performances of angle estimation of the frequency-domain smoothing and non-frequency-domain smoothing, via evaluating the Cramèr-Rao Lower Bounds (CRLBs) associated with the two approaches under the equal transmitted-energy constraint. Such a study is to show the effectiveness of the two smoothing approaches with regard to the estimation performance in an algorithm-independent way for generality of the conclusion. We then compare in Section IV the estimation performance of a typical frequency-domain smoothing algorithm with that of a typical non-frequency-domain smoothing algorithm, using statistical simulations. Section V is devoted to the detection performance comparison, followed by a summary of conclusions and discussions in Section VI.

II. DATA SET MODELING

Two signaling schemes are used in this paper. The frequency-domain smoothing approach uses a frequency diversity signaling, while the non-frequency-domain smoothing approach uses a conventional (no diversity) signaling.

A. Frequency Diversity Signaling

We consider the following simple frequency diversity signaling as illustrated in Fig. 1, where each subpulse of width $\tau' = \tau/J$ has a different carrier frequency with an arbitrary narrowband modulation of its own. For convenience of presentation we assume that the carrier frequencies f_j, $j = 1,2,...,J$ are uniformly spaced, i.e., $f_{j+1} - f_j = \Delta f$ and that all subpulses have the same modulation.

We consider a linear array of M wideband sensors covering the frequency band over which the frequency diversity signaling is used. A sequence of N identical pulses, each of which contains J subpulses as in Fig. 1, is transmitted and reflected by fluctuating targets. Assuming that the d targets in the same range cell and with the same Doppler frequency shift have little range change over a time interval of $(N - 1)$/pulse-repetition frequency (PRF), and that J matched filters are used at all M sensors for preprocessing, we have for each of the N pulses, a set of J $M \times 1$ data vectors for processing over this range cell in the form of

$$x_j = A_j s_j + w_j, \qquad j = 1,2,...,J \qquad (1)$$

where A_j, $M \times d$, is the direction matrix at the frequency f_j, s_j, $d \times 1$, the target complex amplitude vector at f_j and w_j, $M \times 1$, the noise component from the M sensor receivers of the jth subband [1].

We assume that the frequency separation Δf is chosen to be large enough such that s_j, $j = 1,2,...,J$ are statistically independent [14], and that w_j, $j = 1,2,...,J$ have zero mean and the same correlation matrix $\sigma^2 I$, where I denotes the $M \times M$ identity matrix. Both w_j and s_j are modeled as complex normal vectors in this paper. The target fluctuation is assumed to lead to the independence of the N samples of x_j which are identically distributed. Thus, the data set for processing consists of N independent identically distributed (IID) samples of x_j, $j = 1,2,...,J$, i.e., a total of $N \times J$ $M \times 1$ vectors. We note that x_j, $j = 1,2,...,J$ are not statistically identically distributed since A_j, $j = 1,2,...,J$ depend on the carrier frequencies f_j, $j = 1,2,...,J$.

Define the signal-to-noise ratio (SNR) at the jth subband for the kth target as

$$SNR_j(k) = E\{|s_j(k)|^2\}/var\{w_j(m)\},$$

$$j = 1,2,...,J, \quad k = 1,2,...,d. \qquad (2)$$

For convenience of discussion we assume here that the mean-square reflection power of the target does not depend on the carrier frequency, i.e., $E\{|s_j(k)|^2\}$ independent of j. Since $var\{w_j(m)\} = \sigma^2$, we have

$$SNR_j(k) = SNR(k), \qquad j = 1,2,...,J. \qquad (3)$$

We concentrate on the cases of two completely correlated targets ($d = 2$) with different angles of arrival (AOAs) $\theta_1 \neq \theta_2$ and the second arriving signal being a delayed version of the first, i.e.,

$$s_2(t) = \rho s_1(t - t_0) \qquad (4)$$

where ρ is a real constant and t_0 the path delay much smaller than that of the range cell. Let $\phi_j(1)$ and $\phi_j(2)$, $j = 1,2,...,J$ be the phases of the target complex amplitudes $s_j = [s_j(1)\ s_j(2)]^T$ at f_j. From (4) it is seen that

$$\phi_j(2) = \phi_j(1) - 2\pi f_j t_0, \qquad j = 1,2,...,J \qquad (5)$$

i.e., $\phi_j(1)$ and $\phi_j(2)$ are linked by a constant, in contrast to the two independent target reflection cases where $\phi_j(1)$ and $\phi_j(2)$ can be modeled as independent random variables.

For convenience of discussion we assume that the sensors are identical and uniformly spaced with separation $D = \lambda_0/2$ where λ_0 is the wavelength corresponding to f_0, the central frequency of the whole frequency band. The array reference point is chosen to be the center of the aperture with all AOAs referenced to the broadside of the linear array. The Rayleigh angular resolution limit of such an array is about $\Omega = 2/M$ rad.
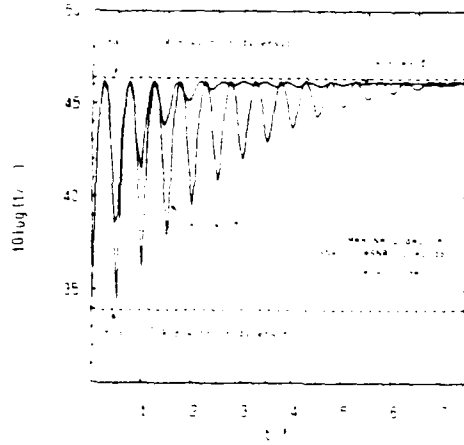
Fig. 2 CRLBs $(10\log_{10}(1/\sigma_\omega^2))$ with frequency diversity:
completely correlated targets.

B. Conventional Signaling

A conventional (no diversity) signaling is assumed
for the non-frequency-domain smoothing approach,
which has a single carrier frequency f_0 for the whole
pulse with an arbitrary narrowband modulation,
i.e., $J = 1$. Therefore, the data set for processing
consists of N $M \times 1$ IID vectors. Imposing the equal
transmitted-energy constraint on both signaling
schemes, we have the SNR with conventional signaling

$$\text{SNR}_0(k) = 10\log J + \text{SNR}(k), \qquad (dB),$$
$$k = 1,2,\ldots,d \qquad (6)$$

i.e., $10\log J$ higher than that with frequency diversity
signaling. We assume that all other conditions and
assumptions on targets and array remain the same
for the performance comparison of the two smoothing
approaches.

III. ESTIMATION PERFORMANCE BOUND
COMPARISON

Since there are many ways to implement smoothing
with either approach, a comparison in terms of some
performance bound is necessary for the generality
of the conclusions on the potentials of the two
approaches. A well-known estimation performance
bound is the CRLB which is relatively easy to evaluate.
It is well known that CRLB bounds the unbiased
estimators only. Though a modified CRLB for biased
estimators is available [15, ch. 4], it is in general
a very difficult task to evaluate the required bias
function of the specific estimator. Since no available
method, to the knowledge of the authors, has been
reported to have a mean-square-error (MSE) below
the corresponding CRLB and since the CRLB can be
fairly tight for SNRs above a certain threshold even
if the data set is small, the use of the CRLB for the
purpose mentioned above is justified.

For a real, jointly normal distributed data set, the
Fisher information matrix for bound calculation can be
expressed as [16]

$$[\mathbf{J}(\theta)]_{u,v} = \frac{1}{2}\text{tr}\left[\mathbf{R}^{-1}(\theta)\frac{\partial \mathbf{R}(\theta)}{\partial \theta_u}\mathbf{R}^{-1}(\theta)\frac{\partial \mathbf{R}(\theta)}{\partial \theta_v}\right]$$
$$+ \left[\frac{\partial \mathbf{m}(\theta)}{\partial \theta_u}\right]^H \mathbf{R}^{-1}(\theta)\left[\frac{\partial \mathbf{m}(\theta)}{\partial \theta_v}\right]$$

where $\mathbf{R}(\theta)$ is the covariance matrix as a function of
the parameter set vector θ, $\mathbf{m}(\theta)$ the mean vector as
a function of θ, and θ_u, θ_v denote the uth and vth
parameter, respectively. For a jointly complex-normal
distributed data set, the above equation can be
modified as

$$[\mathbf{J}(\theta)]_{u,v} = \text{tr}\left[\mathbf{R}^{-1}(\theta)\frac{\partial \mathbf{R}(\theta)}{\partial \theta_u}\mathbf{R}^{-1}(\theta)\frac{\partial \mathbf{R}(\theta)}{\partial \theta_v}\right]$$
$$+ 2\text{Re}\left\{\left[\frac{\partial \mathbf{m}(\theta)}{\partial \theta_u}\right]^H \mathbf{R}^{-1}(\theta)\left[\frac{\partial \mathbf{m}(\theta)}{\partial \theta_v}\right]\right\} \qquad (7)$$

with $\text{Re}(\cdot)$ being the real part of a complex number.
In the case of two completely correlated targets,
the unknown parameters of the data set with a
conventional signaling are the two spatial frequencies

$$\omega_k = 2\pi(D/\lambda_0)\sin\theta_k, \qquad k = 1,2 \qquad (8)$$

the signal power σ_{s1}^2 and σ_{s2}^2, the noise power σ^2, and
the phase difference between the two signals which
depends on the delay t_0. The unknown parameters
with frequency diversity signaling include the signal
powers $\sigma_{s1}^2(j),\sigma_{s2}^2(j)$, noise power $\sigma^2(j)$, $j = 1,2,\ldots,J$,
the delay t_0, and two target AOA related parameters.
We still use ω_1 and ω_2 for these two parameters
since the spatial frequencies at f_j, $j = 1,2,\ldots,J$ are
deterministic functions of these two even if f_0 is not
necessarily equal to one of f_j, $j = 1,2,\ldots,J$.

Let σ_ω^2 be the CRLB to the variance of an ω_1
or ω_2 estimate. In the remainder of this paper and
Figs. 2–5, the abbreviation CRLB is used to denote
$10\log_{10}(1/\sigma_\omega^2)$ as a rather common practice.

We consider the situations where $\rho = 1$ and t_0 is
corresponding to a small fraction of the range cell, i.e.,
$t_0 \ll 1/B'_{max}$, where B'_{max} denotes the largest bandwidth
of the subpulses. In practice, these situations are
found to be the most important and difficult to
handle [10, ch. 3 and 4]. Fig. 2 shows the CRLBs
as a function of $t_0 f_0$ for $J = 7$ subbands with the
relative bandwidth $B/f_0 = 10$ percent and 30 percent,
respectively. The CRLBs oscillate with a damping
factor proportional to B/f_0 but settle at a level
independent of B/f_0. In contrast, the dotted lines
in Fig. 2 indicate the maximum and minimum of the
CRLB for the non-frequency-domain smoothing, which
would oscillate in between with the period equal to
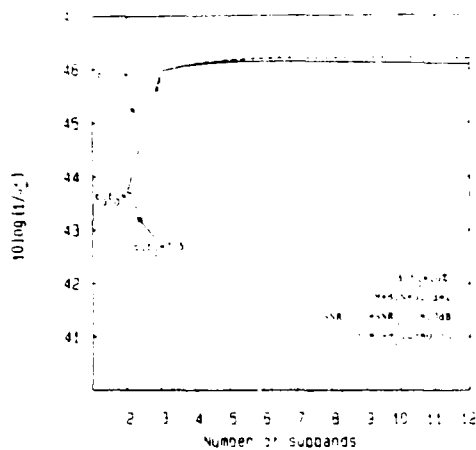0.5. From this figure, we can see that the CRLB for

3

Fig. 3. CRLBs ($10\log_{10}(1/\sigma_\omega^2)$) with frequency diversity versus number of subbands J: completely correlated targets, $B/f_0 = 10$ percent.
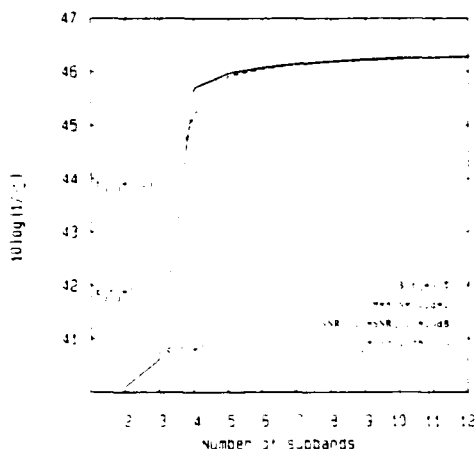

Fig. 4. CRLBs ($10\log_{10}(1/\sigma_\omega^2)$) with frequency diversity versus number of subbands J: completely correlated targets, $B/f_0 = 30$ percent.

the frequency-domain smoothing can be independent of $t_0 f_0$ as long as enough bandwidth is used. For the example of $B/f_0 = 30$ percent, when $t_0 f_0 \geq 2.5$ the bound stays at a level close to the best value of the bound for the non-frequency-domain smoothing. And for $B/f_0 = 10$ percent, the bound gets into the stable region for $t_0 f_0 \geq 7.5$.

The effects of the number of subbands J on the CRLB for the frequency-domain smoothing approach can be seen from Figs. 3 and 4 for the two completely correlated targets with $B/f_0 = 10$ percent and 30 percent, respectively. With small J the CRLBs still depend on the values of $t_0 f_0$. When J is large enough, however, the CRLBs can settle at a level independent of $t_0 f_0$. Moreover, a slightly larger J is needed with larger relative bandwidth B/f_0 for the CRLB to become independent of $t_0 f_0$.

From the above study of CRLBs for the two approaches we can conclude the following.

1) The potential AOA estimation performance of the frequency-domain smoothing approach is expected to always be better than that of the non-frequency-domain smoothing approach.

2) The larger the bandwidth, the better the potential AOA estimation performance can be of the frequency-domain smoothing approach.

3) Only a small number of subbands J are necessary for the potential AOA estimation performance of the frequency-domain smoothing approach to be independent of the unknown delay t_0.

In the next section we study the estimation performances of a typical frequency-domain smoothing method and a typical non-frequency-domain smoothing method.

IV. ESTIMATION PERFORMANCE OF TWO SMOOTHING METHODS

For simplicity we choose the MUSIC-based coherent signal-subspace processing method described in [11, 17] and the MUSIC-based spatial smoothing method of [4]. Since there is little analytical result available about the estimation performance of the spatial smoothing method, we conduct the comparison via statistical simulation. The following parameters are set up for the simulation.

1) the number of targets $d = 2$ with $\rho = 1$, i.e., SNR(1) = SNR(2);

2) the relative bandwidth $B/f_0 = 30$ percent with the number of subbands $J = 7$;

3) the number of sensors $M = 8$;

4) the spatial frequencies $\omega_1 = 0.8227$ and $\omega_2 = 0.430$ which correspond to an angle separation equal to 0.5Ω;

5) the subarray size $L = 6$ for the spatial smoothing method in [4];

6) the required preliminary estimate of approximate center of the spatial frequencies with the frequency-domain smoothing method of [11] $\beta = (\omega_1 + \omega_2)/2$;

7) the equal transmitted-energy constraint as of (6);

8) the number of pulses $N = 32$.

Fig. 5 compares the mean square errors (MSEs) of the two smoothing methods for $\hat\omega_1$ at various SNR with $t_0 f_0 = 6$, 6.25, and 6.5, respectively. Again, $10\log_{10}(1/\text{MSE})$ is actually plotted. Fifty independent runs are used at each SNR. The MSEs of frequency-domain smoothing with the three different values of $t_0 f_0$ are found to be approximately the same and thus only the one with $t_0 f_0 = 6$ is plotted in Fig. 5. Also included in Fig. 5 are the corresponding CRLBs. The frequency-domain smoothing method is seen to significantly outperform the spatial smoothing method,
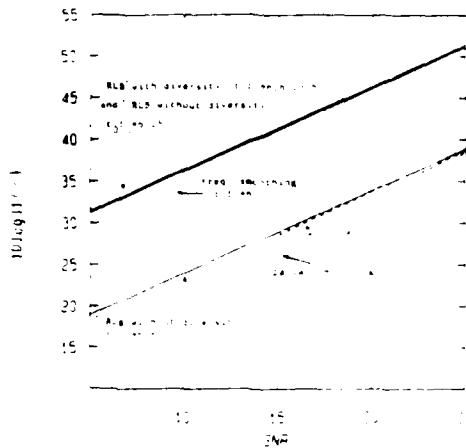
Fig. 5. MSEs of $\hat{\omega}_1$ with frequency-domain smoothing $(B/f_0 = 30$ percent, $J = 7)$ and spatial smoothing versus SNR: completely correlated targets, $M = 8$, $d = 2$, $\omega_1 = 0.8227$, $\omega_2 = 0.430$, $L = 6$, $N = 32$.
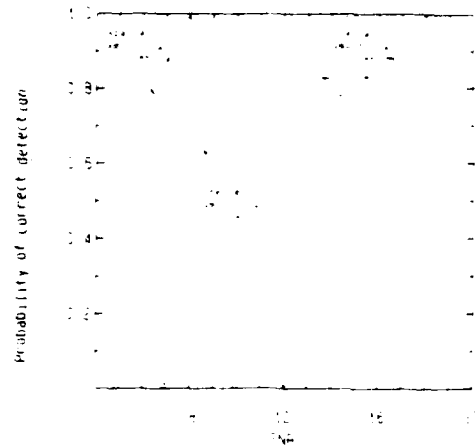

Fig. 6. Detection performances of spatial smoothing and frequency-domain smoothing methods: completely correlated targets, $M = 8$, $d = 2$, $\omega_1 = 0.822\overline{}$, $\omega_2 = 0.430$, $L = 6$, $N = 32$.

and reaches the CRLBs quite closely. We note that with $t_0 f_0 = 6.25$ the spatial smoothing method fails to reach the corresponding CRLB even at very high SNRs. A possible cause of this may stem from the fact that with this spatial smoothing method, not all of the off-diagonal elements of the estimated correlation matrix can be made use of.

Since the frequency-domain smoothing method needs a preliminary estimate β, it is interesting to know its effect on the MSE. It has been shown in [17, 18] that the performance of the frequency-domain smoothing approach is not sensitive to this preliminary estimate.

V. DETECTION PERFORMANCE COMPARISON

The above two MUSIC based smoothing methods both need to first determine the number of targets d before performing AOA or spatial frequency estimation. One may use AIC or MDL types of methods [19, 20] to conveniently accomplish this. For completely correlated targets, [21] gives a spatial smoothing based modification of the AIC/MDL method, while a frequency-domain smoothing based modification is presented and analyzed in [17]. In this section we compare the probability of correct determination of the number of targets with the two modified methods for two completely correlated, closely spaced fluctuating targets under the constraint of equal transmitted-energy. An analytical detection performance study can be found in [17] for the frequency-domain smoothing based method, but a corresponding study for the spatial smoothing based method is not available to our knowledge. Therefore, we conduct the detection performance comparison via simulation. The parameters used in this simulation are the same as those in the last section. Since the probability of underestimating the number of targets

is the dominant detection error for the cases of completely correlated and/or closely spaced signals, and since our previous experience with detection performance analysis has resulted in favor of choosing the AIC rather than MDL penalty function [17, 22, 23], we use the AIC penalty function here.

Fig. 6 shows the probability of correctly determining the number of targets with the spatial smoothing based method [21] and frequency-domain smoothing based method [17] under equal transmitted-energy constraint, using 50 independent runs. In this figure, the probabilities for the spatial smoothing based method with $t_0 f_0 = 6$, 6.25, and 6.5, respectively, are plotted as a function of SNR. For the frequency-domain smoothing based method, the corresponding three curves are almost the same. So only the one with $t_0 f_0 = 6$ is included. The detection performance of the spatial smoothing based method is very sensitive to the values of $t_0 f_0$ (or the phase difference $\phi = 2\pi t_0 f_0$). Though the detection performance of the frequency domain based method is measured about 2 dB poorer in terms of SNR than the spatial smoothing based method with $t_0 f_0 = 6.5$, it performs significantly better than the other two cases of the spatial smoothing based method. Therefore, one may conclude that the frequency-domain smoothing based detection method is more able to provide a well-performed solution for determination of the number of completely correlated, closely spaced fluctuating targets.

VI. CONCLUSION AND DISCUSSION

For high-resolution active direction finding of completely correlated fluctuating targets the results are in favor of using the frequency-domain smoothing approach, which consists of the frequency diversity signaling and a coherent wideband processing

algorithm such as the one described in [11, 17], rather than the non-frequency-domain smoothing approach which uses the conventional (no diversity) signaling ... a narrowband processing algorithm such as the spatial smoothing method of [4, 21]. The study of the estimation performance bounds also indicate that the frequency-domain smoothing can be expected to achieve a much better performance than any non-frequency-domain smoothing, especially for an array with a small number of sensors. We note that for nonfluctuating targets, [24] contains a study which leads to the same conclusion in favor of using the frequency-domain smoothing. We also note that the frequency-domain smoothing can be used with arrays of non-uniformly-spaced, non-identical sensors. It should be pointed out that passive direction finding of completely correlated wideband sources has been successfully solved by using the idea of the frequency-domain smoothing [11, 17].

REFERENCES

[1] Wang, H., Li, C. C., and Zhu, J.-X. (1987)
High-resolution direction finding in the presence of multipath: A frequency-domain smoothing approach.
In *Proceedings of the IEEE International Conference on Acoustics, Speech, and Signal Processing*, Dallas, TX, 1987, 53.5.1–53.5.4.

[2] Gabriel, W. F. (1980)
Spectral analysis and adaptive array superresolution techniques.
Proceedings of the IEEE, 68 (1980), 654–666.

[3] Evans, J. E., Johnson, J. R., and Sun, D. F. (1982)
Application of advanced signal processing technique to angle of arrival estimation in ATC navigation and surveillance systems.
Technical Report 582, Lincoln Laboratory, M.I.T., Lexington, MA, 1982.

[4] Shan, T. J., Wax, M., and Kailath, A. (1985)
On spatial smoothing for direction of arrival estimation of coherent signals.
IEEE Transactions on Acoustics, Speech, and Signal Processing, ASSP-33, 4 (Aug. 1985), 806–811.

[5] Kung, S. Y., Lo, C. K., and Foka, R. (1986)
A Toeplitz approximation approach to coherent source direction finding.
In *Proceedings of the IEEE International Conference on Acoustics, Speech, and Signal Processing*, Tokyo, Japan, 1986, 5.7.1–5.7.4.

[6] Takao, K., Kikuma, N., and Yano, T. (1986)
Toeplitzization of correlation matrix in multipath environment.
In *Proceedings of the IEEE International Conference on Acoustics, Speech, and Signal Processing*, Tokyo, Japan, 1986, 35.15.1–35.15.4.

[7] Haber, F., and Zoltowski, M. (1986)
Spatial spectrum estimation in a coherent signal environment using an array in motion.
IEEE Transactions on Antennas and Propagation, AP-34, 3 (Mar. 1986), 301–310.

[8] Schmidt, R. O. (1981)
A signal subspace approach to multiple emitter location and spectral estimation.
Ph.D. dissertation, Standford University, Standford, CA, Nov. 1981.

[9] Zoltowski, M., and Haber, F. (1986)
A vector space approach to direction finding in a coherent multipath environment.
IEEE Transactions on Antennas Propagation, AP-34, 9 (Sept. 1986), 1069–1079.

[10] Haykin, S. (1985)
Radar array processing for angle of arrival estimation.
In S. Haykin (Ed.), *Array Signal Processing* Englewood Cliffs, NJ: Prentice-Hall, 1985, ch. 4, 194–292.

[11] Wang, H., and Kaveh, M. (1985)
Coherent signal-subspace processing for the detection and estimation of angles of arrival of multiple wide-band sources.
IEEE Transactions on Acoustics, Speech, and Signal Processing, ASSP-33, 4 (Aug. 1985), 823–831.

[12] Wang, H., and Kaveh, M. (1984)
Estimation of angles of arrival for wide-band sources.
In *Proceedings of the IEEE International Conference on Acoustics, Speech, and Signal Processing*, San Diego, CA, 1984, 7.5.1–7.5.4.

[13] Hung, H., Wang, H., and Kaveh, M. (1986)
Further results on coherent signal-subspace processing.
In *Proceedings of the 3rd ASSP Workshop on Spectrum Estimation and Modeling*, (Nov. 1986), 97–100.

[14] Van Trees, H. L. (1968)
Detection Estimation and Modulation Theory, Part III.
New York: Wiley, 1968, 418–419.

[15] Zacks, S. (1971)
The Theory of Statistical Inference.
New York: Wiley, 1971.

[16] Porat, B., and Friedlander, B. (1986)
Computation of the exact information matrix of Gaussian time series with stationary random components.
IEEE Transactions on Acoustics, Speech, and Signal Processing, ASSP-34, 1 (Feb. 1986), 118–130.

[17] Wang, H., and Kaveh, M. (1987)
On the performance of signal-subspace processing—Part II: coherent wideband systems.
IEEE Transactions on Acoustics, Speech, and Signal Processing, ASSP-35, 11 (Nov. 1987), 1583–1591.

[18] Wang, H., and Kaveh, M. (1985)
Sensitivity and performance analysis of coherent signal-subspace processing for multiple wideband sources.
In *Proceedings of the IEEE International Conference on Acoustics, Speech, and Signal Processing*, Tampa, FL, 1985, 17.6.1–17.6.4.

[19] Wax, M., and Kailath, T. (1983)
Estimating the number of signals by information theoretic criteria.
In *Proceedings of the 2nd ASSP Workshop on Spectrum Estimation and Modeling*, Tampa, FL, 1983, 192–196.

[20] Bai, Z. D., Krishnaiah, P. R., and Zhao, L. C. (1987)
On estimation of the number of signals and frequencies of multiple sinusoids.
In *Proceedings of the IEEE International Conference on Acoustics, Speech, and Signal Processing*, Dallas, TX, 1987, 30.5.1–30.5.4.

[21] Shan, T. J., Paulraj, A., and Kailath, T. (1986)
On smoothed rank profile tests in eigenstructure approach to direction of arrival estimation.
In *Proceedings of the IEEE International Conference on Acoustics, Speech, and Signal Processing*, Tokyo, Japan, 1986, 35.24.1–35.24.4.

[22] Wang, H., and Kaveh, M. (1986)
On the performance of signal-subspace processing—Part I narrow-band systems.
IEEE Transactions on Acoustics, Speech, and Signal Processing, ASSP-34, 5 (Oct. 1986), 1201–1209.

[23] Kaveh, M., Wang, H., and Hung, H. (1987)
       On the theoretical performance of a class of estimators of
       the number of narrowband sources.
       *IEEE Transactions on Acoustics, Speech, and Signal
       Processing*, ASSP-35, 9 (Sept. 1987), 1350-1352.
[24] Wang, H., and Zhu, J. X. (1988)
       On performance improvement of tone frequency
       estimation in active radar and sonar systems:
       non-fluctuating targets.
       *IEEE Transactions on Acoustics, Speech, and Signal
       Processing*, ASSP-36, 10 (Oct. 1988), 1582-1591.

Jian-Xiong Zhu (S'88) was born in Jiangsu, China on March 8, 1965. He received
the B.S. degree in electrical engineering from the University of Science and
Technology of China, Hefei, China, in 1985. He is now a Ph.D. student at Syracuse
University, Syracuse, New York.

He has been a Research Assistant at Syracuse University since 1987. His
current research interests are in array signal processing, spectral estimation, and
digital signal processing.

Hong Wang (S'83—M 85) received the Ph.D. degree in electrical engineering from
the University of Minnesota, Minneapolis, in 1985.

He joined the Faculty of the Department of Electrical and Computer
Engineering at Syracuse University, Syracuse, New York, in 1985, where he is
currently an Assistant Professor. His research interest is signal processing with its
applications to radar and sonar systems.

Dr. Wang is the recipient of the 1989 IEEE Acoustics, Speech, and Signal
Processing Society's Paper Award.

Some remarks on the above analysis are in order now.

Remark 1: Since the estimate $\hat{P}(\omega_1, \omega_2)$, given by (4), (8), and (9), satisfies condition 1) for $(l, k) \in \Omega$ and condition 2) for $|k| > K$, respectively, we can conclude that the estimate $\hat{P}(\omega_1, \omega_2)$ given by Kimura and Honoki's hybrid approach coincides with the true ME estimate when $\hat{\Pi}_a(\omega_1)$ is positive definite, and the elements of the first row of its inverse $\hat{\Pi}_a^{-1}(\omega_1)$ satisfy (26).

Remark 2: If the original estimate $\hat{\Pi}(\omega_1)$ is of Toeplitz, $\hat{\Pi}(\omega_1)$ is directly taken as $\hat{\Pi}_a(\omega_1)$; in the other case, $\hat{\Pi}_a(\omega_1)$ is obtained by averaging $\hat{\Pi}(\omega_1)$, see [1, eq. (20)]. In a way similar to our above analysis, it can be straightforwardly concluded that for a multichannel process $X(t)$, the power spectrum estimate $\hat{\Pi}_a(\omega_1)$ is the true ME estimate when every element $[\hat{\Pi}_a^{-1}(\omega_1)]_{ij}$ of the inverse $\hat{\Pi}_a^{-1}(\omega_1)$ has the form of $\Sigma_{l=-L}^{L} C_l^{ij} \exp(j\omega_1 l)$ for $|l| > L$. This can be regarded as another form of (26) for the multichannel 1-D process. It is worthwhile to point out even if the estimate $\hat{\Pi}_a(\omega_1)$ is the true ME estimate, the final estimate $\hat{P}(\omega_1, \omega_2)$ obtained by using $\hat{\Pi}_a(\omega_1)$ is not necessarily the ME estimate, as will be stated in the next remark.

Remark 3: Since the positivity of $\hat{\Pi}_a(\omega_1)$ is available for the case of cyclic and skew-cyclic Toeplitz $R(l)$, Kimura and Honoki have conjectured that their final estimate $\hat{P}(\omega_1, \omega_2)$ coincides with the true ME estimate for such a case. The above analysis conclusion shows that Kimura and Honoki's conjecture is not true in general since the cyclic and skew-cyclic Toeplitz $R(l)$ cannot, in general, guarantee that all the elements of the first row of the inverse $\hat{\Pi}_a^{-1}(\omega_1)$ satisfy (26). To show this point, we present a counterexample of Kimura and Honoki's conjecture.

It is always possible to find a multichannel process $X(t)$ such that it has the following power spectrum:

$$\hat{\Pi}(\omega_1) = \begin{bmatrix} \dfrac{5 + 2\cos\omega_1}{25 + 20\cos\omega_1 + 4\cos(2\omega_1)} & \dfrac{-2\sin\omega_1}{25 + 20\cos\omega_1 + 4\cos(2\omega_1)} \\[3mm] \dfrac{-2\sin\omega_1}{25 + 20\cos\omega_1 + 4\cos(2\omega_1)} & \dfrac{5 + 2\cos\omega_1}{25 + 20\cos\omega_1 + 4\cos(2\omega_1)} \end{bmatrix}$$

$$= \begin{bmatrix} f_{11}(\omega_1) & f_{12}(\omega_1) \\ f_{21}(\omega_1) & f_{22}(\omega_1) \end{bmatrix} \tag{27}$$

By using definition (11a), it is easy to show $\hat{\Pi}(\omega_1)$ is of cyclic Toeplitz. Since there are $f_{11}(\omega_1) = f_{22}(\omega_1)$ and $f_{12}(\omega_1) = f_{21}(\omega_1)$ between the elements of $\hat{\Pi}(\omega_1)$, we see that

$$R(l) = \frac{1}{2\pi} \int_{-\pi}^{\pi} \hat{\Pi}(\omega_1) \exp(j\omega_1 l) \, d\omega_1$$

is also of cyclic Toeplitz. Hence, $\hat{\Pi}(\omega_1)$ is directly taken as $\hat{\Pi}_a(\omega_1)$, and

$$\hat{\Pi}_a^{-1}(\omega_1) = \hat{\Pi}^{-1}(\omega_1) = \begin{vmatrix} 5 + 2\cos\omega_1 & 2\sin\omega_1 \\ 2\sin\omega_1 & 5 + 2\cos\omega_1 \end{vmatrix}. \tag{28}$$

Note that the given $\hat{\Pi}(\omega_1)$ is positive definite and is simply shown to be the ME estimate (cf. Remark 2) and the corresponding $R(l)$ is of cyclic Toeplitz, but the final spectrum estimate $\hat{P}(\omega_1, \omega_2)$ obtained by Kimura and Honoki's hybrid approach from such $\hat{\Pi}(\omega_1)$ does not coincide with the true ME estimate since for the case of $k = 0$ and $|l| > L$,

$$\sum_m \frac{b_{0m}(\omega_1) b_{0n}^*(\omega_1)}{b_{0n}^*(\omega_1)}$$

$$= \frac{b_{01}(\omega_1) b_{01}^*(\omega_1) + b_{00}(\omega_1) b_{00}^*(\omega_1)}{b_{00}^*(\omega_1)}$$

$$= 5 + 2\cos\omega_1 + \frac{4\sin^2\omega_1}{5 + 2\cos\omega_1}$$

is the sum of infinite terms; this implies that

$$\int_{-\pi}^{\pi} \int_{-\pi}^{\pi} \frac{\exp[j(\omega_1 l + \omega_2 k)]}{\hat{P}(\omega_1, \omega_2)} \, d\omega_1 \, d\omega_2 \neq 0,$$

for $k \leq K, |l| > L.$

IV. CONCLUSIONS

Some important theoretical problems remain to be solved in Kimura and Honoki's hybrid approach to high-resolution 2-D spectrum analysis. The most important problem is probably to know when the final estimate is close to the true ME estimate. In this correspondence, we have analyzed such a problem, and our work has provided a "theoretical" and "practical" solution to this problem. Using our result, one can easily know if the final estimate given by Kimura and Honoki's hybrid approach does coincide with the true ME estimate.

We have also presented a counterexample, and have shown that Kimura and Honoki's conjecture on the above problem is not true.

REFERENCES

[1] H. Kimura and Y. Honoki, "A hybrid approach to high resolution two-dimension spectrum analysis," *IEEE Trans. Acoust., Speech, Signal Processing*, vol. ASSP-35, pp. 1024–1036, July 1987.

[2] D. E. Dudgeon and R. M. Mersereau, *Multidimensional Digital Signal Processing*. Englewood Cliffs, NJ: Prentice-Hall, 1984.

[3] S. Hankin, Ed., *Nonlinear Methods of Spectral Analysis*. New York: Springer-Verlag, 1983.

Adaptive Beamforming for Correlated Signal and Interference: A Frequency Domain Smoothing Approach

J. X. ZHU AND H. WANG

Abstract—This correspondence suggests a new approach to wideband adaptive beamforming for correlated signal and interference. Unlike other approaches, such as spatial smoothing, the new approach solves the signal cancellation problem by employing the idea of frequency domain smoothing. Advantages of frequency domain smoothing over spatial smoothing are identified in this correspondence. Preliminary performance studies of a simple frequency domain smoothing method show that proper spatial filtering can be achieved by frequency domain smoothing, whether the desired signal and the interference are correlated or not.

I. INTRODUCTION

Signal cancellation is a problem of adaptive beamforming (ABF) when the desired signal from the look direction and the interference are highly correlated. One cure is the so-called spatial smoothing method [1], by which the full sensor array is divided into partially overlapping subarrays to enable an average of the covariance matrices of the subarray output vectors. Such an average was shown to be able to destroy the correlation between the signal and interference. Unfortunately, spatial smoothing can only be applied to arrays of uniformly spaced, identical sensors. Besides, a tradeoff has to be made for a given array between the size of the subarrays and the number of subarrays, since the interference rejection performance with spatial smoothing depends on both parameters. Moreover, if the number of sensors is not large enough, the number of subarrays available for spatial smoothing might be too small to lead to any significant improvement.

A rather different approach for wide-band ABF is given in [2], which does not suffer from the signal cancellation since it employs the "complete nulling" criterion at every subband. Such a criterion, however, may sacrifice too much signal power, resulting in an array output signal-to-interference-plus-noise ratio (SINR) lower than that potentially achievable, especially when the interference sources are not very strong and their angles of arrival are close to that of the desired signal [3].

In this correspondence, we present a new approach to wide-band ABF for correlated signal and interference. The key idea is to perform a smoothing operation in the frequency domain, which was originally presented in the context of high-resolution direction finding of multiple wide-band sources [4].

Fig. 1 shows a general configuration of a frequency domain implementation of wide-band bandpass ABF. For simplicity of presentation, we consider a linear array. The sensors do not need to be uniformly spaced, nor do their patterns need to be identical. Following each sensor is a bank of J narrow-band filters covering the whole frequency band of interest. The bandwidth of each subband is assumed to be a few percent of its central frequency f_j, $j = 1, 2, \cdots, J$ so that for each subband, the narrow-band array output representation is valid. The ABF weight vectors w_j, $j = 1, 2, \cdots, J$ are updated according to the chosen optimization criterion and interference environment. Several criteria all result in the form of

$$w_j = \alpha_j R_{jj}^{-1} a_j(\theta_L) \qquad j = 1, 2, \cdots, J \qquad (1)$$

where α_j is a criterion dependent constant, R_{jj} is the correlation matrix of the complex output vector $x_j(t)$ of the jth subband array, and $a_j(\theta_L)$ is the jth subband array direction vector at the look angle θ_L. When the interference is completely or partially correlated to the desired signal from θ_L, the signal cancellation occurs and the claimed optimum performance is completely lost due to the violation of the basic assumption.

It should be pointed out that if the existence of the correlation between the signal and interference is known in advance, then one should take advantage of the signal-correlated interference to achieve an even higher SINR, instead of simply trying to suppress all interference [5]. However, such a priori knowledge is not always available, nor always easy to obtain from the received data. Therefore, the need still remains for finding w_j, $j = 1, 2, \cdots, J$ such that the interference suppression performance is much better than that using (1) when the signal and interference are correlated, and close to that using (1) when the signal and interference are not correlated.

In the following discussion we assume:

1) the angle of arrival of the desired signal θ, is available and used as the array look direction θ_L;

2) the interference sources, correlated or uncorrelated with the desired signal, occupy the same frequency band as the desired signal; and
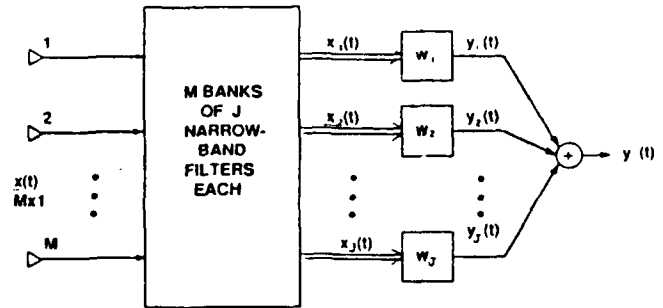
3) the receiver noise is uncorrelated sensor to sensor.

Fig. 1. Configuration of frequency decomposed wide-band beamformer

II. FREQUENCY DOMAIN SMOOTHING

It is easy to see that the correlation matrix of the jth subband array output has the form

$$R_{jj} = A_j R_j A_j^H + \sigma_j^2 I \qquad (2)$$

where A_j, $M \times d$, $d \leq M$ is the direction matrix associated with the desired signal and $d - 1$ interference sources; R_j, $d \times d$ is the correlation matrix of the desired signal and interference; and $\sigma_j^2 I$ is the correlation matrix of the receiver noise of the jth subband. When there is a complete correlation between the desired signal and an interference source, R_j, $j = 1, 2, \cdots, J$ becomes singular and the so-called signal cancellation occurs.

As pointed out in [4], the frequency-domain-smoothed correlation matrix $R \triangleq \Sigma_{j=1}^{J} R_j$ is nonsingular in general. This fact leads to the opportunity of employing a frequency-domain-smoothed "correlation matrix" to replace R_{jj} of (1), so that the beamformer can deliver a reasonably good spatial filtering performance insensitive to whether the desired signal and interference are (completely) correlated or not.

Parallel to the direction finding problem using the idea of frequency domain smoothing [4], a class of adaptive wide-band beamformers with frequency domain smoothing can be developed for different applications. In this correspondence, however, we are only interested in presenting one example which is suitable for a number of practical applications in radar, sonar, and spread-spectrum communication.

To implement the smoothing operation on R_j, $j = 1, 2, \cdots, J$, a frequency domain transformation represented by T_j must be performed on the estimate of the correlation matrix R_{jj} such that

$$T_j A_j = A_0, \qquad j = 1, 2, \cdots, J \qquad (3)$$

where A_0 is the direction matrix of the array at the central frequency f_0 (f_0 may be equal to one of f_j, $j = 1, 2, \cdots, J$). Obviously, there are many possible choices of T_j which could achieve (3), but all of them would need the angles of arrival of the interference which are not available to the beamforming subsystem. Therefore, approximations of T_j of (3) have to be used in practice.

One possible way is to do a preselected angle approximation to the perfect transformation matrix T_j. Let θ_l be the look direction of the array, and $\theta_m \neq \theta_l$, $m = 1, 2, \cdots, M - 1$ be $M - 1$ different angles uniformly covering the whole angular domain of concern. Conceptually summarized below are the steps used to implement the frequency-domain-smoothed adaptive beamformer with a preselected approximation of the transformation.

1) Form $\hat{R}_{jj}$, the estimate of the correlation matrix R_{jj}, from the K sampled complex output vectors $x_j(t)$, $j = 1, 2, \cdots, J$;

2) perform the frequency domain transformation to obtain

$$\hat{R}_s = \sum_{j=1}^{J} \hat{T}_j \hat{R}_{jj} \hat{T}_j^H \qquad (4)$$

where

$$\hat{T}_j = A_0 A_j^{-1} \qquad (5)$$

with

$$A_i = \left[a_i(\theta_i) \mid a_i(\theta_1) \; a_i(\theta_2) \cdots a_i(\theta_{M-1}) \right]; \qquad (6)$$

3) form the frequency-domain-smoothed "correlation matrix" estimate for each subband

$$\check{R}_{ij} \doteq (\hat{T}_j^{-1}) \hat{R}_i (\hat{T}_j^{-1})^H. \qquad (7)$$

4) obtain the beamforming weight vector for the jth subband

$$w_j = \check{R}_{ij}^{-1} a_j(\theta_i), \qquad j = 1, 2, \cdots, J. \qquad (8)$$

We note that significant reduction in computing for $\hat{T}_j$ and $\hat{T}_j^{-1}$ can be expected by exploiting the structure of A_i. In the following section, we will present our preliminary performance study of the above method.

III. PRELIMINARY PERFORMANCE STUDY

In this section we will show the beam patterns of both frequency domain smoothing and spatial smoothing. For simplicity, we consider an array of $M = 10$ uniformly spaced, omnidirectional sensors with the space between sensors equal to one-half of the wavelength corresponding to f_0, and we assume that the desired signal, interference, and receiver noise all have flat spectra in the same frequency band with a relative bandwidth $B/f_0 = 0.30$. The whole band is covered by $J = 10$ subbands. The angle of arrival of the desired signal is taken to be $\theta_i = 35°$. Two interference sources are present. The first one is completely correlated with the desired signal, being a delayed version with delay $t_0 = 15/f_0$. The second interference source is a strong jammer which is uncorrelated with the desired signal. The angles of arrival of the two interference sources are $20°$ and $50°$, respectively.

In Fig. 2, the solid line is the beam pattern of the frequency domain smoothing method. The two dashed lines are the beam patterns of the spatial smoothing method with the subarray size equal to 4 and 6, respectively; and the beam pattern without any smoothing is plotted as the dotted line. The protection of frequency domain smoothing against both interference sources is seen to be much better than that of spatial smoothing.

Since the beam pattern of frequency domain smoothing is the sum of the J subband beam patterns, the sharp null at the angle of the strong interference indicates that the J subband beam patterns must have nulls almost at the same angle even though the transformation used is just an approximation.

Comparing the two beam patterns of spatial smoothing, one can see that the protection against the correlated interference can be gradually improved by reducing the size of the subarrays. Such a reduction of the subarray size for more spatial smoothing not only is limited by the number of interference sources, but also degrades the nulling performance at the angle of the strong interference due to the loss of angular resolution with the reduced subarray size [6]. In contrast, frequency domain smoothing is free from this problem as shown in Fig. 2.

If the interference exists only over *part* of the frequency band, (7) and (8) indicate that this frequency domain smoothing method will produce nulls in *all* J subband beam patterns toward the partial-band interference. To avoid such unnecessary nulls in the interference-free subbands, one may simply apply Steps 1)-4) to those subbands containing interference, and use the conventional beamforming method for the interference-free subbands. If the interference sources have a colored spectrum, a more sophisticated method of frequency domain smoothing needs to be developed.

IV. CONCLUSION

The frequency domain smoothing approach suggested in this correspondence can outperform the spatial smoothing approach,
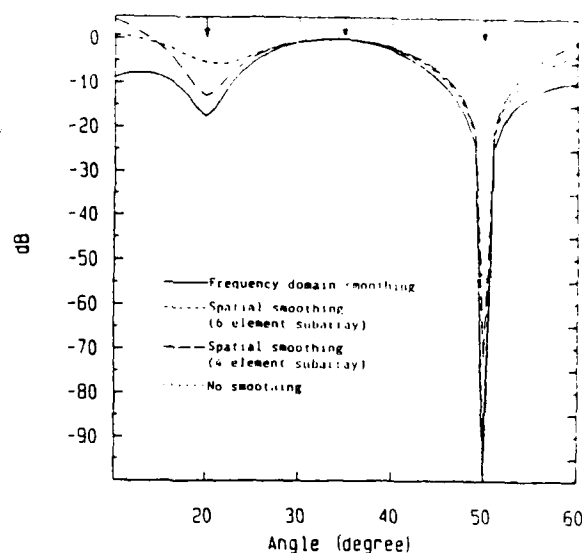

Fig. 2. Beam patterns of the frequency domain smoothing method and spatial smoothing method.

especially for small sensor arrays. The features of this new approach include the following:

1) it can be applied to arrays with arbitrary geometry and sensor patterns;

2) it does not sacrifice the angular resolution for smoothing; and

3) it does not need a large number of sensors to effect the smoothing operation.

We note that [2], [7], and [8] contain some interesting results on the construction of the approximations to the linear transform of (3).

REFERENCES

[1] T. J. Shan and T. Kailath, "Adaptive beamforming for coherent signals and interference," *IEEE Trans. Acoust., Speech, Signal Processing*, vol. ASSP-33, pp. 527-536, June 1985.

[2] J. F. Yang and M. Kaveh, "Wideband adaptive arrays based on the coherent signal-subspace transformation," in *Proc. IEEE Int. Conf. Acoust., Speech, Signal Processing*, Dallas, TX, Apr. 1987, pp. 47.6.1-47.6.4.

[3] H. C. Lin, "Spatial correlations in adaptive arrays," *IEEE Trans. Antennas Propagat.*, vol. AP-30, pp. 212-223, Mar. 1982.

[4] H. Wang and M. Kaveh, "Coherent signal-subspace processing for the detection and estimation of angles of arrival of multiple wide-band sources," *IEEE Trans. Acoust., Speech, Signal Processing*, vol. ASSP-33, pp. 823-831, Aug. 1985.

[5] Y. Bresler, V. U. Reddi, and T. Kailath, "A polynomial approach to optimum beamforming for correlated or coherent signal and interference," in *Proc. IEEE Int. Conf. Acoust., Speech, Signal Processing*, Dallas, TX, Apr. 1987, pp. 53.9.1-53.9.4.

[6] I. J. Gupta and A. A. Ksienski, "Dependence of adaptive array performance on conventional array design," *IEEE Trans. Antennas Propagat.*, vol. AP-30, pp. 549-553, July 1982.

[7] H. Hung and M. Kaveh, "Focusing matrices for coherent signal subspace processing," submitted to *IEEE Trans. Acoust., Speech, Signal Processing*.

[8] K. M. Buckley and L. J. Griffiths, "BASS-ALE estimation for broadband sources and focussing transformation evaluation," in *Proc. 21st Asilomar Conf. Signals, Syst., Comput.*, Pacific Grove, CA, Nov. 1987.

Effects of Sensor Position and Pattern Perturbations on CRLB
For Direction Finding of Multiple Narrow-Band Sources

J.X. Zhu and H. Wang

Department of Electrical & Computer Engineering
Syracuse University
Syracuse, NY 13244-1240

ABSTRACT

This paper studies the effects of sensor pattern and sensor position perturbations on the angle estimation performance bound for multiple narrow-band sources. The Cramer-Rao Lower Bound is used with a probabilistic modeling of the perturbations. The CRLBs of a linear uniform array under sensor position and pattern perturbations are evaluated in detail for the case of two narrow-band sources.

I.   INTRODUCTION

In many applications where a sensor array is used for angle estimation of multiple sources/targets, one has to consider the effects of the sensor pattern and sensor position perturbations. Though some efforts have been made to develop robust high-resolution estimates [1]-[3], there is a need to understand the behavior of the estimation performance bound under the perturbations, so that one can see how much room left for developing more robust estimate.

In this paper, the behavior of estimation performance bound under sensor position and pattern perturbations is investigated. The Cramer-Rao Lower Bound (CRLB) is chosen since it is simple to evaluate, and since all available high-resolution direction finding methods require either large number of snapshots or high SNR, for which the CRLB has been seen to provide a reasonably tight bound on the mean-square-error (MSE) of the angle estimate. The perturbations on sensor positions and patterns are modeled as Gaussian random variables. We note that previous work on evaluation of the CRLB under perturbations, such as [4]-[6], involves the cases of single source and multiple sources disjoint in the frequency domain.

II.   MODEL FORMULATION

Consider an array with arbitrary but known nominal geometry as shown in Fig.1. Let the number of sensors be M, each at position $\vec{p}_1=(x_1\ y_1)$, $\vec{p}_2=(x_2\ y_2)$, ..., $\vec{p}_M=(x_M\ y_M)$, with respect to the chosen reference point. Denote the sensor pattern of the m-th sensor as $g_m(\theta)$. Let $\vec{v}_1$,

$\vec{v}_2,...,\vec{v}_d$ be the wave-number vectors of d narrow-band plane waves of the same central frequency f_0. The array output complex vector $\underline{X}$, Mx1, can be expressed as

$$\underline{X} = \Lambda \underline{S} + \underline{N} \qquad (1)$$

where $\Lambda = [\underline{a}_1\ \underline{a}_2\ ...\underline{a}_d]$ is the direction matrix with the direction vector

$$\underline{a}_i = [g_1(\theta_i)\exp\{j2\pi\vec{p}_1(-\vec{v}_i)\},$$
$$g_2(\theta_i)\exp\{j2\pi\vec{p}_2(-\vec{v}_i)\},$$
$$.......$$
$$g_M(\theta_i)\exp\{j2\pi\vec{p}_M(-\vec{v}_i)\}]^T, \quad i=1,2,...,d, \quad (2)$$

$\underline{S} = [S_1\ S_2\ ...\ S_d]^T$ the arriving signal vector modeled as zero-mean Gaussian random vector with a diagonal covariance matrix, and $\underline{N} = [N_1\ N_2\ ...\ N_M]^T$ the receiver noise modeled as zero-mean Gaussian random vector with its covariance matrix equal to $\sigma_n^2 I$. $\underline{S}$ and $\underline{N}$ are assumed to be independent.

From Fig.1, we have

$$\vec{p}_m(-\vec{v}_i) = (x_m\cos\theta_i + y_m\sin\theta_i)/\lambda ,$$
$$m=1,2,...,M, \quad i=1,2,...,d. \quad (3)$$

In the presence of sensor position perturbation, the m-th sensor position vector becomes $\vec{p}_m=(x_m+\Delta x_m\ \ y_m+\Delta y_m)$, where Δx_m and Δy_m are the sensor position perturbations in x direction and y direction respectively. The sensor position perturbations Δx_m, Δy_m, m=1,2,...,M are modeled as i.i.d. Gaussian random variables of zero mean. We assume that the standard deviation of the position perturbations is much smaller than the spaces among the sensors.

The perturbed complex gains, i.e., the perturbed sensor patterns, are modeled as $g_m(\theta)+\Delta g_m(\theta)$ where $g_m(\theta)$, m=1,2,...M are the nominal patterns and $\Delta g_m(\theta)$, m=1,2,...M, are i.i.d. zero mean complex Gaussian random perturbations. Again, the standard deviation is assumed to be much smaller than the nominal complex gain $g_m(\cdot)$.

In order to see the amplitude and phase perturbation effects separately, a model for the case of pattern amplitude perturbation only is also set up, in which the nominal pattern $g_m(\theta)$,

$m=1,2,\ldots,M$ are assumed to be positive and the perturbations $\Delta g_m(\theta)$, $m=1,2,\ldots,M$ to be i.i.d real zero mean Gaussian random variables.

When multiple snapshots are used for estimation, the independence of snapshots is assumed and the perturbations are assumed to remain unchanged among all snapshots.

III. CRAMER-RAO LOWER BOUND UNDER PERTURBATIONS

If we only consider position perturbations, i.e., assume no pattern perturbations, then the unknown real parameter set θ contains

$$\theta = (\theta_1 \ \theta_2 \ \ldots \ \theta_d \ \sigma_{s1}^2 \ \sigma_{s2}^2 \ \ldots \ \sigma_{sd}^2 \ \sigma_n^2$$
$$\Delta x_1 \ \Delta y_1 \ \Delta x_2 \ \Delta y_2 \ \ldots \ \Delta x_M \ \Delta y_M) \quad , \qquad (4)$$

i.e., a total of $2d+1+2M$ real parameters. For the case of pattern perturbations only, the unknown real parameter set θ is

$$\theta = (\theta_1 \ \theta_2 \ \ldots \ \theta_d \ \sigma_{s1}^2 \ \sigma_{s2}^2 \ \ldots \ \sigma_{sd}^2 \ \sigma_n^2$$
$$Re(\Delta g_1(\theta_1)) \ Im(\Delta g_1(\theta_1)) \ \ldots \ Re(\Delta g_1(\theta_d)) \ Im(\Delta g_1(\theta_d))$$
$$Re(\Delta g_2(\theta_1)) \ Im(\Delta g_2(\theta_1)) \ \ldots \ Re(\Delta g_2(\theta_d)) \ Im(\Delta g_2(\theta_d))$$
$$\ldots\ldots\ldots\ldots$$
$$Re(\Delta g_M(\theta_1)) \ Im(\Delta g_M(\theta_1)) \ \ldots \ Re(\Delta g_M(\theta_d)) \ Im(\Delta g_M(\theta_d)))$$
$$(5)$$

a total of $2d+1+2Md$ real parameters. For the case of pattern amplitude perturbations only, $\Delta g_m(\theta)$, $m=1,2,\ldots,M$ are set up as i.i.d. real zero mean Gaussian random variables in section II. Therefore the unknown real parameter set in this case is

$$\theta = (\theta_1 \ \theta_2 \ \ldots \ \theta_d \ \sigma_{s1}^2 \ \sigma_{s2}^2 \ \ldots \ \sigma_{sd}^2 \ \sigma_n^2$$
$$\Delta g_1(\theta_1) \ \Delta g_1(\theta_2) \ \ldots \ \Delta g_1(\theta_d)$$
$$\Delta g_2(\theta_1) \ \Delta g_2(\theta_2) \ \ldots \ \Delta g_2(\theta_d)$$
$$\ldots\ldots\ldots\ldots$$
$$\Delta g_M(\theta_1) \ \Delta g_M(\theta_2) \ \ldots \ \Delta g_M(\theta_d)) \qquad (6)$$

a total of $2d+1+Md$ real parameters.

With the presence of random parameters, the Fisher information matrix is given by [7]

$$\underline{J}(\theta) = \underline{J}_1(\theta) + \underline{J}_2(\theta) \qquad (7)$$

where the elements of $\underline{J}_1$ and $\underline{J}_2$ are

$$[\underline{J}_1(\theta)]_{i,j} = -E_{X,\theta}\left(\frac{\partial^2 \log(Pr(X|\theta))}{\partial\theta_i\partial\theta_j}\right) \qquad (8)$$

$$[\underline{J}_2(\theta)]_{i,j} = -E_\theta\left(\frac{\partial^2 \log(Pr(\theta))}{\partial\theta_i\partial\theta_j}\right) \quad . \qquad (9)$$

Under the assumption that the position and pattern perturbations are small, $\underline{J}_1(\theta)$ can be approximated by the corresponding Fisher information matrix for non-random θ at the nominal values [4], i.e.,

$$[\underline{J}_1(\theta)]_{i,j} \simeq -E_X\left(\frac{\partial^2 \log(Pr(X|\theta))}{\partial\theta_i\partial\theta_j}\right)\Big|_{\theta=\theta_0} \qquad (10)$$

where θ_0 is the parameter set at the nominal value. For Gaussian signals and noises Eq. (10) becomes [4]

$$[\underline{J}_1(\theta)]_{i,j} = tr\left[\underline{R}^{-1}(\theta)\frac{\partial R(\theta)}{\partial\theta_i}\underline{R}^{-1}(\theta)\frac{\partial R(\theta)}{\partial\theta_j}\right]\Big|_{\theta=\theta_0} \qquad (11)$$

where $\underline{R}$ is the covariance matrix of the data vector $\underline{X}$.

Because the first $2d+1$ parameters are non-random, $\underline{J}_2(\theta)$ has it's first $2d+1$ rows and columns equal to zero. Let $\Lambda_{p(2M\times2M)}$ be the covariance matrix of the position perturbations, $\Lambda_{g(2Md\times2Md)}$ the covariance matrix of the pattern perturbations (real and imaginary part), and $\Lambda_{a(Md\times Md)}$ the covariance matrix of the pattern amplitude perturbation. For sensor position perturbation only, we have

$$\underline{J}_2(\theta) = \left[\begin{array}{c|c} 0_{2d+1 \times 2d+1} & 0 \\ \hline 0 & \Lambda_{p(2M\times2M)}^{-1} \end{array}\right] , \qquad (12)$$

and for pattern perturbation only, we have

$$\underline{J}_2(\theta) = \left[\begin{array}{c|c} 0_{2d+1 \times 2d+1} & 0 \\ \hline 0 & \Lambda_{g(2Md\times2Md)}^{-1} \end{array}\right] , \qquad (13)$$

and for pattern amplitude perturbation only,

$$\underline{J}_2(\theta) = \left[\begin{array}{c|c} 0_{2d+1 \times 2d+1} & 0 \\ \hline 0 & \Lambda_{a(Md\times Md)}^{-1} \end{array}\right] . \qquad (14)$$

In the case of multiple snapshots, the probability density function $Pr(X|\theta)$ in Eq.(8) would be joint density function $Pr(X_1,X_2,\ldots X_K|\theta)$, where K is the number of snapshots. Under the assumption that all snapshots are independently identically distributed, $Pr(X_1,X_2,\ldots X_K|\theta) = [Pr(X_1|\theta)]^K$ and Eq.(8) becomes

$$[\underline{J}_1(\theta)]_{i,j} = -K\cdot E_{X,\theta}\left(\frac{\partial^2\log(Pr(X_1|\theta))}{\partial\theta_i\partial\theta_j}\right) \qquad (15)$$

The $\underline{J}_2(\theta)$ will remain the same as in Eq.(9) because of the assumption that the perturbations remain unchanged among all snapshots.

In the following section, we will numerically evaluate the CRLB for a linear uniform array to see how the sensor position and pattern perturbations affect the estimation bound.

IV. CASE STUDY

We consider an array of 8 sensors with half wavelength spacing, which presents a Rayleigh angular resolution of $16.4°$ (degree). For simplicity, the nominal sensor patterns are assumed to be omnidirectional, i.e., $g(\theta)=1$ for all sensors. Let θ_1 and θ_2 be the angles of arrival of two narrow band sources of the same central frequency. Again, for simplicity, we fix θ_1 at

12

$0°$, and then $\Delta\theta = \theta_2-\theta_1 = \theta_2$. In the following figures, the CRLB for θ_2 estimation under pattern amplitude, pattern amplitude and phase, and position perturbations, denoted as CRLBa, CRLBg and CRLBp respectively, are compared with the CRLB for θ_2 estimation without perturbations (CRLB$_0$). For pattern amplitude perturbations the standard deviation is denoted as σ_a. For pattern amplitude and phase perturbations, which are modeled as i.i.d. zero mean complex Gaussian random variables, we denote the standard deviation of its real part or imaginary part as σ_g, i.e., the standard deviation of the complex pattern perturbation is $\sqrt{2}\sigma_g$. For sensor position perturbations, we let the standard deviation of the perturbations in x direction and y direction be the same and denoted as σ_p.

Figure 2 shows the effect of the pattern amplitude perturbations on the bound (CRLBa) as a function of $\Delta\theta$, the angular separation between the two narrow-band sources. For $\Delta\theta$ larger than the resolution cell ($=16.4°$), the CRLBa is almost the same as CRLB$_0$, i.e., the amplitude perturbation of the sensor gains has almost no effect on the estimation performance potential. In the high-resolution region ($\Delta\theta < 16.4°$), however, the larger the amplitude perturbation, the poorer the estimation performance potential, which implies some extra difficulty to overcome in order to achieve high resolution.

To overcome such an extra difficulty for high resolution, Fig. 3 shows that one possible way is to increase the signal-to-noise ratio (SNR). In this sense we may loosely consider that the pattern amplitude perturbation has a similar effect on the performance potential as the receiver noise.

Figure 4, Figure 5 and Figure 6 show the CRLB under both the amplitude and phase perturbation on the sensor pattern (CRLBg). When perturbations on the phases of the complex sensor gain are added, the CRLBg behaves quite differently from that without phase perturbation. Figure 4 shows the bound as a function of the angle separation $\Delta\theta$ with different σ_g, while Figure 5 as of SNR with different $\Delta\theta$ and Figure 6 as of SNR with different σ_g. Both Figure 5 and Figure 6 indicate that with the phase perturbations on the sensor gain, the CRLBg will level off as SNR increases. That is, the CRLBg can not be reduced to arbitrarily small by increasing SNR. Under sensor pattern perturbation, therefore, it is the phase perturbation that significantly affects the estimation performance.

Figures 7-9 show the CRLB under sensor position perturbations (CRLBp). We can see that the effects of position perturbation are almost the same as that of pattern perturbation. Again, when noise is no longer a dominant factor, it is the position perturbation that will limit the estimation performance.

Fig. 7 plots CRLBp as a function of the angular separation $\Delta\theta$. In the low-resolution region ($\Delta\theta > 16.4°$), the degradation from the CRLB$_0$ is almost independent of $\Delta\theta$ and determined only by the position perturbation standard deviation σ_p. In the high-resolution region ($\Delta\theta < 16.4°$), however, the degradation from CRLB$_0$ is $\Delta\theta$-dependent and becomes smaller when $\Delta\theta$ is smaller. Noting the sharp increase of CRLB$_0$ in the high-resolution region, we should realize that the smaller degradation with smaller $\Delta\theta$ merely means the more dominant factor which the receiver noise shows with smaller $\Delta\theta$.

Fig. 10 shows the effect of the number of snapshots on the CRLB under position perturbations (CRLBp), from which the increase of the number of snapshots is seen to be similar to the increase of the signal to noise ratio. That is, as the number of snapshots increases the CRLBp levels off.

V. CONCLUSIONS

Both sensor pattern and position perturbation can seriously degrade the potential estimation performance. With proper joint estimation scheme, the effect of the pattern amplitude perturbation might be compensated by increasing the signal to noise ratio. When the signal to noise ratio is high the position perturbation or pattern phase perturbation becomes the dominant factor and the CRLBp or CRLBg will level off. In such situations, one might not be able to reduce the CRLBg and CRLBp to an arbitrarily small number by further increase of the signal to noise ratio, even with some joint estimation scheme. Under the pattern or position perturbation, the increase of the number of snapshots is expected to offer only limited help as the SNR.

REFERENCES

[1] K. M. Buckley, "Incorporated robustness in narrowband signal subspace spatial spectral estimators," Proc. ICASSP'87, pp. 2.7.1-2.7.4, Dallas, TX, 1987.

[2] T. J. Shan, A. M. Bruckstein and T. Kailath, "Multiple signal resolution with uncertain signal space," Proc. 19th Asilomar Conf. Circuits, Systems and Computers, pp. 78-82, Pacific Grove, CA, Nov. 1985.

[3] A. Paulraj and T. Kailath, "Direction of arrival estimation by eigenstructure methods with unknown sensor gain and phase," Proc. ICASSP'85, pp. 640-643, April 1985.

[4] Y. Rockah and P. M. Schultheiss, "Array shape calibration using sources in unknown locations—Part I: Far-field sources," IEEE Trans. Acoust., Speech, Signal Processing, vol. ASSP-35, No.3, pp.286-299, March 1987.

[5] Y. Rockah and P. M. Schultheiss, "Array shape calibration using sources in unknown locations—Part II: Near-field sources," IEEE Trans. Acoust., Speech, Signal Processing,

vol. ASSP-35, No.6, pp.724-735, June 1987.

[6] Y. Rockah, H. Messer and P. M. Schultheiss, "Source localization with an array subject to uncertainty in sensor phases" Proc. Twentieth Annual Conference on Information Sciences and Systems, pp.751-760, Princeton, NJ, 1986.

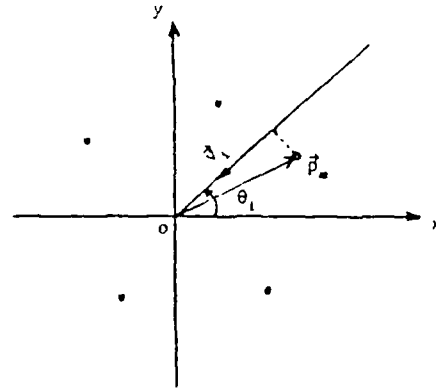[7] H. L. Van Trees, Detection Estimation and Modulation Theory, Part I. New York: Wiley, 1968, p. 84.
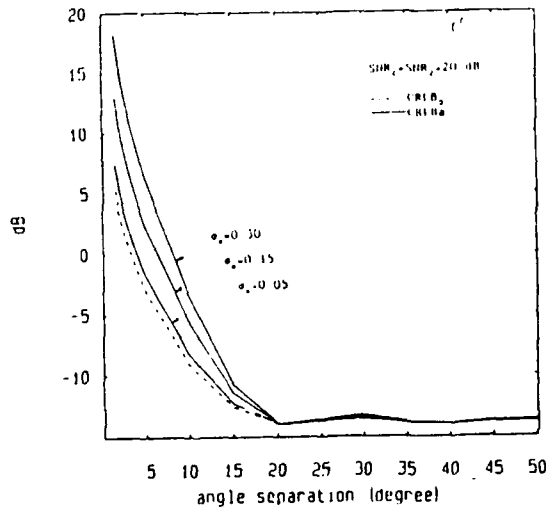
Fig. 1   Problem geometry

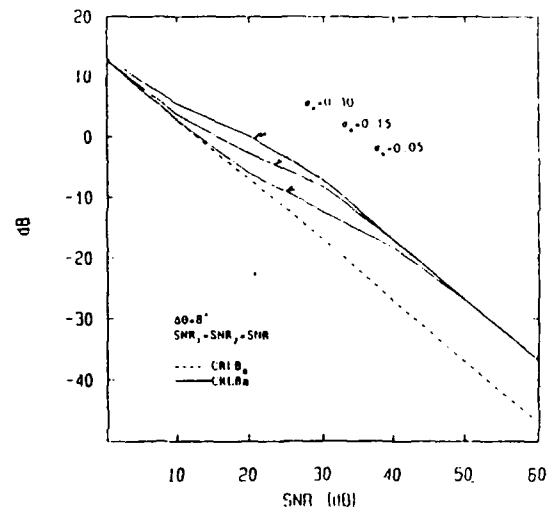Fig 2 CRLB under pattern amplitude perturbations (CRLBa) vs angle separation with different ϕ_a

Fig 3 CRLB under pattern amplitude perturbations (CRLBa) vs. SNR with different ϕ_a
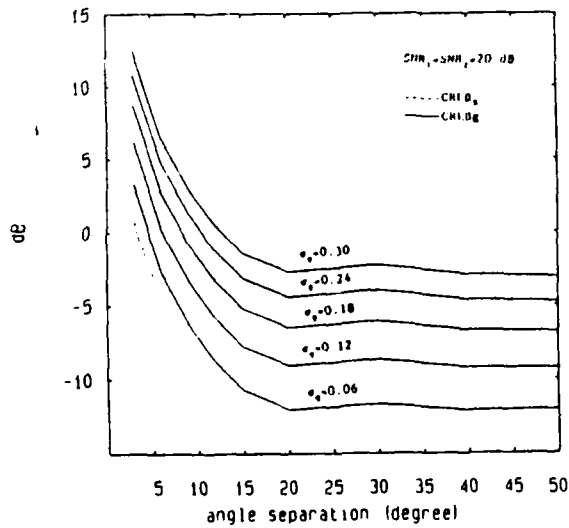
Fig 4 CRLB under pattern perturbations (CRLBg) vs angle separation with different ϕ_g
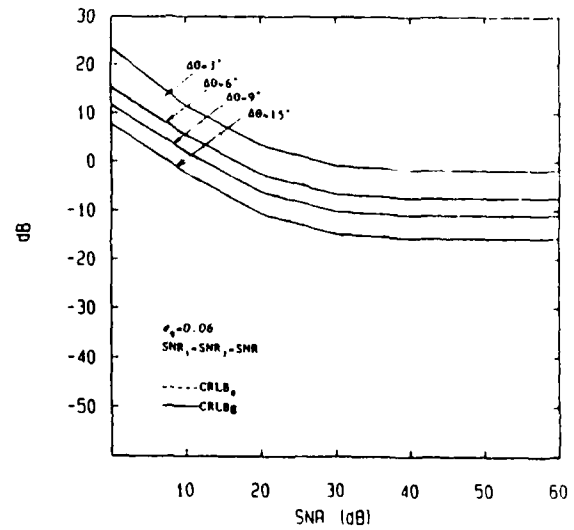
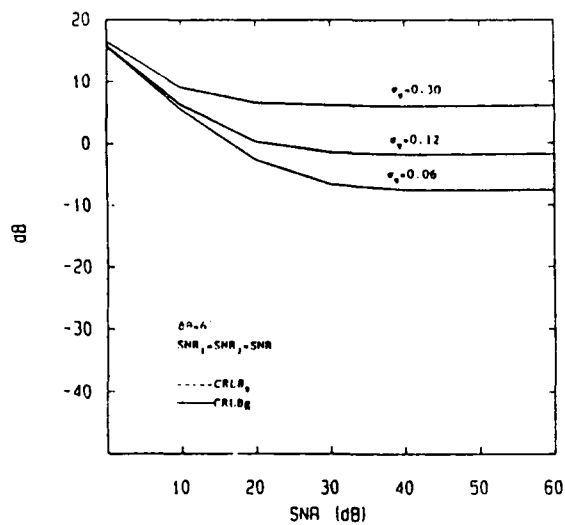Fig 5 CRLB under pattern perturbations (CRLBg) vs SNR with different angle separations

14

Fig. 6 CRLB under pattern perturbations (CRLBg)
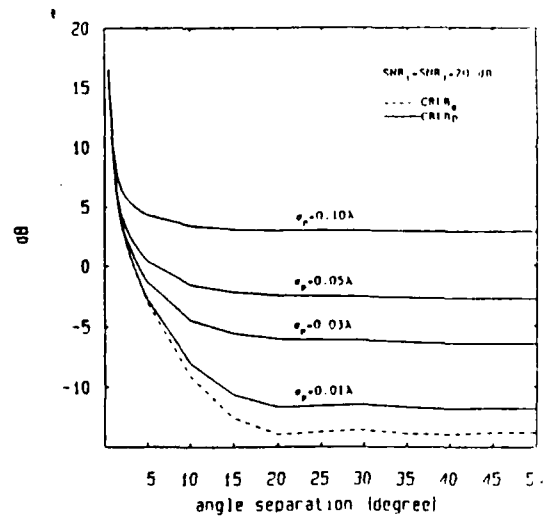vs. SNR with different σ_g

Fig. 7 CRLB under sensor position perturbations (CRLBp)
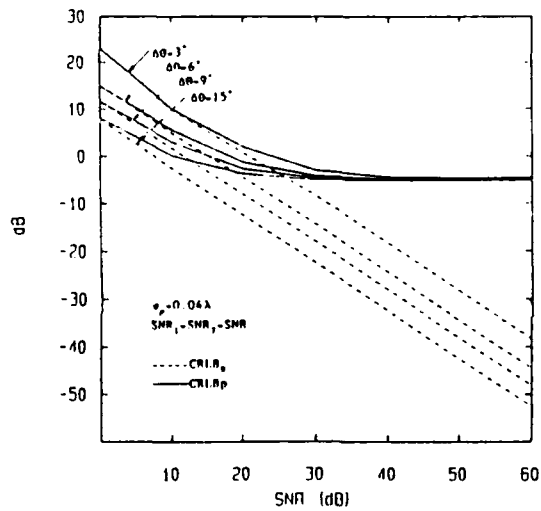vs. angle separation with different σ_p

Fig. 8 CRLB under sensor position perturbations (CRLBp)
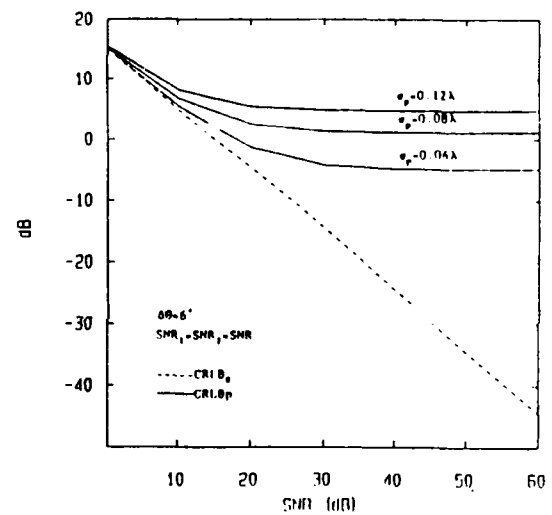vs. SNR with different angle separation

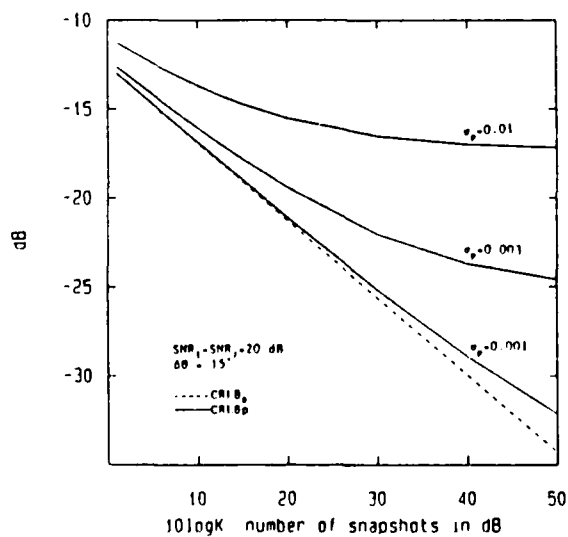Fig. 9 CRLB under sensor position perturbations (CRLBp)
vs. SNR with different σ_p

Fig. 10 CRLB under sensor position perturbations (CRLBp)
vs. number of snapshots with different σ_p

15

MISSION

of

Rome Air Development Center

RADC plans and executes research, development, test and selected acquisition programs in support of Command, Control, Communications and Intelligence (C^3I) activities. Technical and engineering support within areas of competence is provided to ESD Program Offices (POs) and other ESD elements to perform effective acquisition of C^3I systems. The areas of technical competence include communications, command and control, battle management information processing, surveillance sensors, intelligence data collection and handling, solid state sciences, electromagnetics, and propagation, and electronic reliability/maintainability and compatibility.